Densities of Liquid Tm_2O_3, Yb_2O_3, and Lu_2O_3 Measured by an Electrostatic Levitation Furnace Onboard the International Space Station

Takehiko Ishikawa [1,2,*], **Chihiro Koyama** [1], **Hirohisa Oda** [1], **Rina Shimonishi** [1], **Tsuyoshi Ito** [1] **and Paul-François Paradis** [3]

[1] Japan Aerospace Exploration Agency, Tsukuba 305-8505, Japan; koyama.chihiro@jaxa.jp (C.K.); oda.hirohisa@jaxa.jp (H.O.); shimonishi.rina@jaxa.jp (R.S.); ito.tsuyoshi@jaxa.jp (T.I.)

[2] Department of Space and Astronautical Science, SOKENDAI (The Graduate University for Advanced Studies), Sagamihara 252-5210, Japan

[3] Institut National d'Optique, Quebec City, QC G1P 4S4, Canada; paul-francois.paradis@ino.ca

[*] Correspondence: ishikawa.takehiko@jaxa.jp; Tel.: +81-70-1170-2788

Abstract: Liquid densities of three lanthanoid sesquioxides (Tm_2O_3, Yb_2O_3, and Lu_2O_3), whose melting temperatures are above 2400 °C, were measured using an electrostatic levitation furnace onboard the International Space Station (ISS). Each sample was positively charged, and its position was controlled by Coulomb forces between the sample and the surrounding electrodes. Following heating and melting of the sample by high-power lasers, its volume was calculated from its spherical shape in its liquidus phase. After weighing the mass of the sample returned to Earth, its density was determined. The densities (ρ) of Tm_2O_3, Yb_2O_3, and Lu_2O_3 can be expressed as $\rho_{Tm2O3} = 8304 - 0.18 \times (T - T_m)$, $\rho_{Yb2O3} = 8425 - 0.55 \times (T - T_m)$, and $\rho_{Lu2O3} = 8627 - 0.43 \times (T - T_m)$, respectively, where T_m is their melting temperatures.

Keywords: levitation; high-temperature melts; lanthanoid sesquioxides; density

1. Introduction

As the additive manufacturing (3D printing) techniques progress with ceramics materials [1], demands for the measurement of the thermophysical properties of oxide melts are increasing [2]. However, due to their high melting temperatures and the risk of contamination from walls, thermophysical property measurements of molten oxides with conventional techniques such as crucibles are difficult. Among oxides, molten lanthanoid sesquioxides (Ln_2O_3, where Ln = La, Ce, Pr, Nd, Sm, Eu, Gd, Tb, Dy, Ho, Er, Tm, Yb, and Lu) are very hard to investigate due to their extremely high melting temperatures (above 2400 °C).

Densities of Ln_2O_3 were measured by direct [2,3] and indirect methods [4]. As for the indirect methods, Courtial and Dingwell measured the density of Na-disilicates, which contained 0 to 6% of Ln_2O_3 and had melting temperatures below 1300 °C, using the double-bob Archimedean method. Then, they obtained a partial molar volume of Ln_2O_3 as a function of the concentration, and this was extrapolated to get the molar volume of 100% Ln_2O_3 [4].

The direct methods utilize containerless processing techniques. These methods circumvent the problems associated with the crucibles and enable the property measurements of high-temperature melts. One of the most common levitation methods for high-temperature material is electromagnetic levitation. It has been widely used for high-temperature melts of metals and alloys on the ground [5–8] as well as in space [9–12]. However, this method cannot handle oxide materials due to their low electric conductivities.

Another method utilizes gas flow to levitate samples. Aerodynamic levitation (ADL) uses a conical nozzle through which a gas flows and creates a stable point (pressure

minimum) where a sample can be levitated. The levitated sample can be heated and melted using high-power lasers. Granier and Heurtault [3] used this method to measure the densities of several Ln_2O_3s.

The aero-acoustic levitator (AAL) levitates a sample with a gas jet and stabilizes it by acoustic forces using surrounding transducers. The sample position is monitored, and the acoustic pressures are adjusted using a feedback control algorithm. The densities of Ln_2O_3s obtained by this method are reported by Ushakov et al. [2].

The electrostatic levitation method (ESL) [13] utilizes Coulomb force between a charged sample and surrounding electrodes to levitate a sample against gravity. In principle, any sample can be handled as long as it has enough charges on its surface. High-temperature melts were successfully levitated electrostatically in the 1990s [14]. Since then, thermophysical properties (density [15], surface tension [16], viscosity [16], and heat capacity [17]) of molten refractory metals/alloys have been measured using this method on the ground [18]. However, levitation of oxide samples with this method on the ground is very challenging due to the following reasons. To levitate a sample (typically a size of 2 mm in diameter and mass of around 30 mg) against gravity, a certain amount of surface charge (around 10^{-10} C) and a huge electric field (10–20 kV/cm) are needed. These requirements can be easily satisfied for conductive samples such as metals/alloys under a high-vacuum environment. However, it is very difficult to accumulate enough electrical charges on the oxide samples. Moreover, the oxide samples need to be processed under a gaseous environment to prevent evaporation, where a huge electric field cannot be applied because electric discharges between electrodes occur easily.

In microgravity, a large electric field is not necessary, and restrictions are drastically relieved, allowing the handling of oxide samples with much fewer electrical charges. Moreover, levitation experiments can be conducted in a gaseous environment. Microgravity is, therefore, a suitable environment for thermophysical property measurements of high-temperature oxide melts with an electrostatic levitation method.

The electrostatic levitation furnace onboard the ISS (ISS-ELF) has been developed by the Japan Aerospace Exploration Agency (JAXA) and has been operational since 2016 [19]. To validate and demonstrate the capability of thermophysical property measurements of molten oxides at extremely high temperatures, Ln_2O_3s have been selected as the main target of the ISS-ELF project. Densities of Gd_2O_3, Tb_2O_3, Ho_2O_3, and Er_2O_3 were successfully measured from 2017 to 2019 and reported in earlier publications [20–22]. Subsequently, densities of Tm_2O_3, Yb_2O_3, and Lu_2O_3 were measured in 2021. This paper briefly describes the facility as well as the measurement method and reports the density data of these Ln_2O_3s.

2. Experimental Setup

2.1. Electrostatic Levitation Furnace

A detailed description of the facility is found in earlier publications [19,20], but a summary is given here for completeness.

A positively charged sample can be levitated among three pairs of electrodes orthogonally located against each other (Figure 1). To achieve this, a collimated laser beam (around 20 mm in diameter) from a diode laser emitting at a wavelength of 660 nm projects a shadow of the sample on a position sensor where vertical and horizontal sample positions are measured. Two sets of the projection lasers and position sensors are orthogonally placed to allow measuring the tridimensional sample position. The position signals are sent to a controller, where the position control voltages are calculated using a PD (proportional-differential) control algorithm.

Figure 1. A positively charged sample levitating among 3 pairs of electrodes in the ISS-ELF.

The sample is heated by four semiconductor lasers (980 nm, 40 W power each) in which beams are focused to a 0.5 mm spot size at the sample position. To maintain good temperature homogeneity of the sample, these lasers are arranged in a tetrahedral heating geometry around the sample. Furthermore, the power of each laser can be controlled by commands from the ground.

The sample temperature is measured at a 100 Hz frequency over the 300 °C to 3000 °C range by a commercial pyrometer (IMPAC IGA140) through sapphire windows. The pyrometer measures the radiation intensity (1.45–1.8 μm in wavelength) from the sample. Because the emissivity setting on the pyrometer cannot be changed from the ground, it remains at 1.0. The actual sample temperature can be determined using the temperature plateau after recalescence and the known melting temperature of the material. The pyrometer contains a built-in video camera that helps ensure that the sample stays in the measuring spot of the pyrometer (Figure 2a).
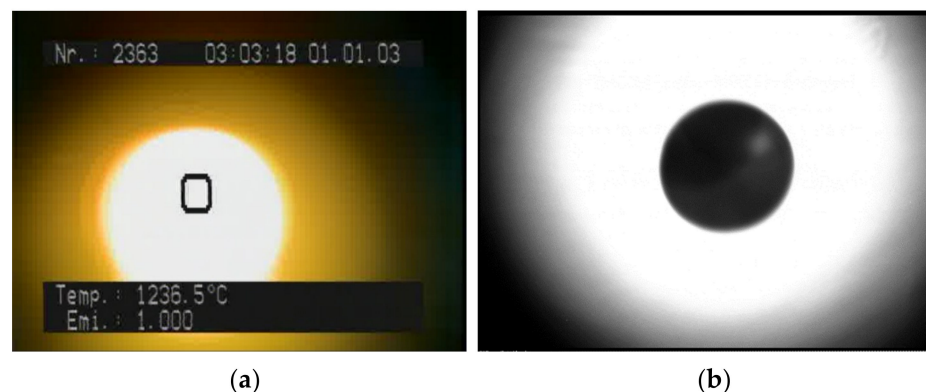

(**a**)   (**b**)

Figure 2. Magnified images of a sample in the ISS-ELF taken by: (**a**) a camera built into the pyrometer (the black square indicates the measuring spot); (**b**) a black and white camera with UV backlighting.

The other camera (a black and white camera with a non-telecentric zoom lens) gives a magnified image of a UV backlit sample (Figure 2b). Using the video images (taken at a 60 Hz frequency interval) from this camera, the density of the sample can be calculated.

Other than the exchanges of sample holders by crew members, all operations of the ISS-ELF are remotely conducted from the ground. Experiments were carried out under a dry air pressurized atmosphere (2×10^5 Pa).

2.2. Density Measurement

Spherical samples were prepared on the ground from compacted powder melted using an aerodynamic levitator in an ambient air atmosphere. Purities and manufacturers of the powders are listed in Table 1. Because these samples (Tm_2O_3, Yb_2O_3, and Lu_2O_3) do not absorb the radiation close to 980 nm, special surface treatments were needed. To achieve this, the spherical samples were aerodynamically levitated and melted in an argon gaseous environment for around 30–60 s so that their surfaces were chemically reduced and covered with a thin metallic layer (Figure 3a). Following this treatment, some of the samples were

heated with a semiconductor laser in a dry air environment, and it was confirmed that the samples could absorb the laser radiation and that the samples temperatures could be raised. This also helped confirm that the samples' surfaces were oxidized again at high temperatures.

Table 1. Source and mass fraction purity of samples used in this study.

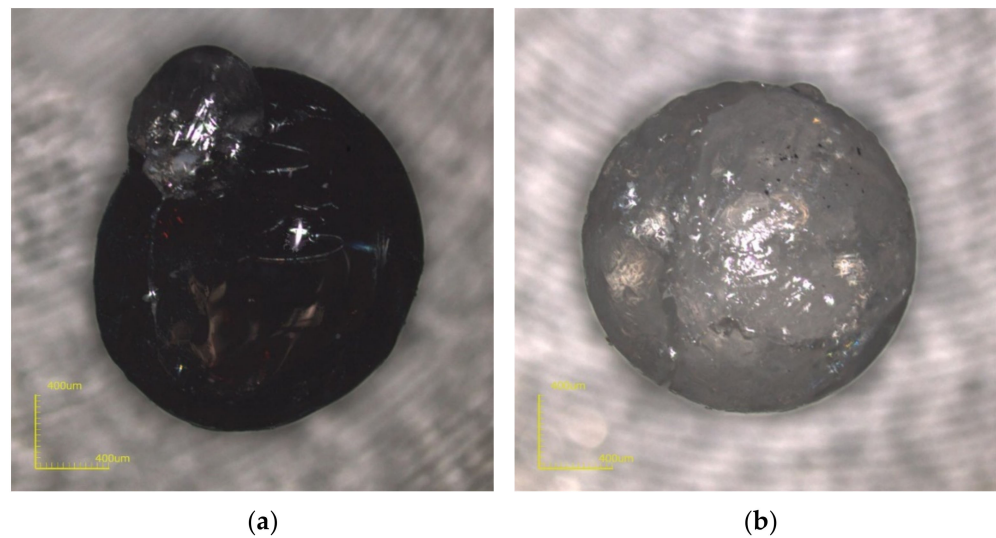| Chemical Name	Source	Initial Mass Fraction Purity
Tm_2O_3	High Purity Chemical Lab.	0.999
Yb_2O_3	High Purity Chemical Lab.	0.9999
Lu_2O_3	High Purity Chemical Lab.	0.999

(**a**)   (**b**)

Figure 3. A Yb_2O_3 sample used for the experiment in the ISS-ELF: (**a**) before flight; (**b**) after flight.

Among 10 samples, 5 samples were selected for each specimen, weighed, inserted in a sample holder, and sent to the ISS.

In the ISS-ELF, a stainless-steel ball (2.0 mm in diameter) was levitated, and its images were taken for the camera calibration. Then, an oxide sample was levitated and heated by the semiconductor lasers. When the sample was successfully melted, the heating lasers were powered off. The sample cooled down, solidified, and then returned back to the sample holder. This process was repeated for all samples in the holder.

After the experiment, still images of the molten samples were captured from the recorded video for image analysis to obtain the sample volume. The detailed method of image analysis is described in Ref. [15]. In short, 400 edge points were detected and converted to polar coordinates (R,θ). Then, these points were fit with the spherical harmonic functions through sixth order as:

$$R(\theta) = \sum_{n=0}^{6} c_n P_n(\cos\theta) \tag{1}$$

where $P_n(\cos\theta)$ are the n-th order Legendre polynomials, and c_n are the coefficients that were determined to minimize the following value:

$$F = \sum_{j=1}^{400} \left\{ R_j - R_j(\theta) \right\}^2 \tag{2}$$

Then, the volume was calculated by the following equation with the assumption that the sample shape is axisymmetric:

$$V = \frac{2\pi}{3} \int_0^\pi R^3(\theta) \sin\theta d\theta \tag{3}$$

The mass (*m*) of the processed sample was weighed once it returned to the ground, allowing to obtain the density from:

$$\rho = \frac{m}{V} \tag{4}$$

The temperature data were corrected using the temperature plateau and the given melting temperatures of the materials with the assumption that the emissivity values of the molten samples remained constant over the temperature range. By synchronizing the time–temperature with time–density data, the density as a function of temperature could be obtained. This density measurement procedure with the ISS-ELF was validated with Al_2O_3 [19].

3. Results and Discussion

In some experiments, the sample position control became unstable during heating due to the sudden reduction of surface charges at high temperatures, which resulted in the loss of samples. Nonetheless, some samples could be successfully melted, and the density data could be obtained.

Figure 4 shows typical time–temperature profiles of the molten samples in their cooling phases. Temperature data were adjusted so that their temperature plateau matched the given melting temperatures [23,24]. Usually, levitated samples reach deeply undercooled temperatures, but these samples did not exhibit such deep undercoolings. Masuno et al. melted Lu_2O_3 samples with an ADL and observed an undercooling of 100 K as well as a double recalescence phenomenon [25]. Such temperature profiles were not obtained in our experiments. They measured the sample temperatures with a very fast pyrometer (with a 100 kHz sampling rate), and their samples were cooled at relatively higher cooling rates than the samples in our experiment (due to gas flow). These differences may be reflected in the difference on the temperature profiles.
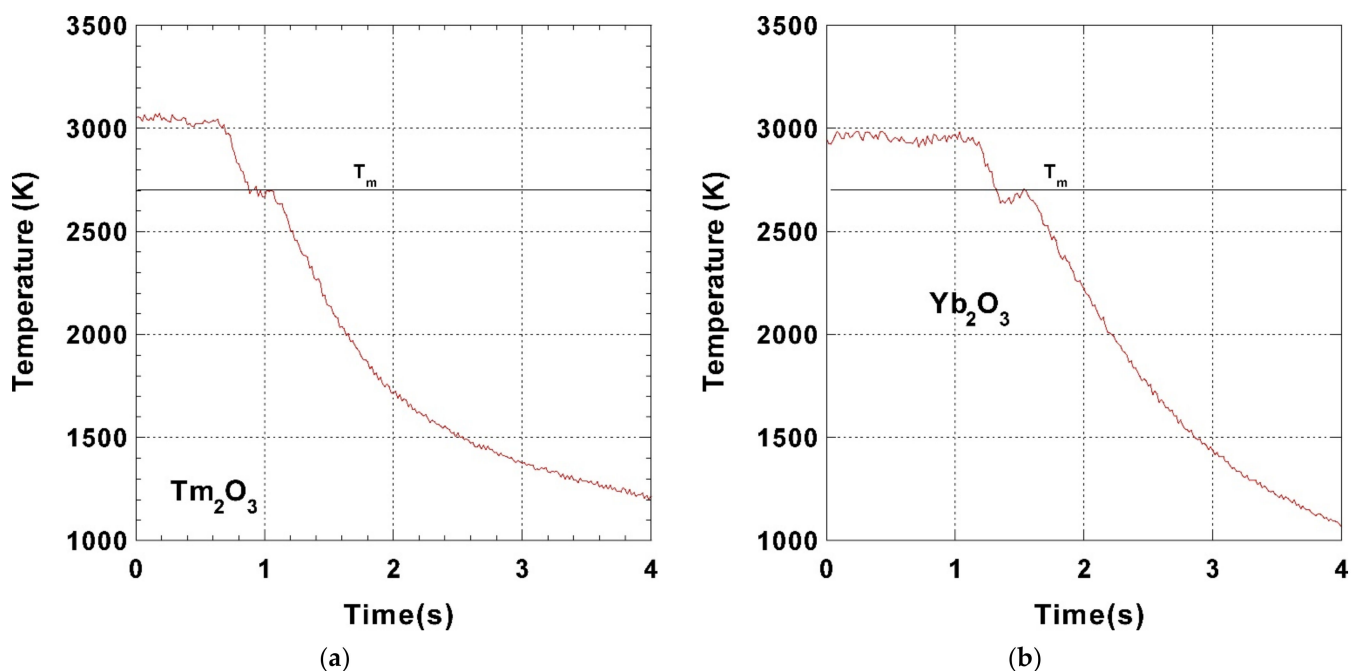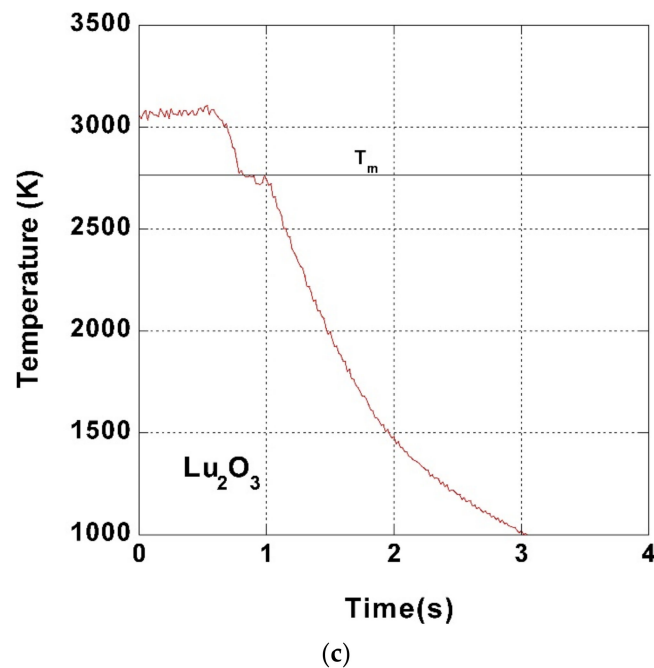

(a)

(b)

Figure 4. *Cont.*

(**c**)

Figure 4. Time–temperature profiles obtained in each Ln_2O_3 sample: (**a**) Tm_2O_3; (**b**) Yb_2O_3; (**c**) Lu_2O_3.

All the samples were successfully recovered and returned to Earth. The samples were entirely white (Figure 3b), indicating that the reduced sample surfaces were oxidized and back to original Ln_2O_3 compositions at high temperatures. Typical sample masses before and after the flight experiments are listed in Table 2. Slight mass losses are identified due to evaporation during the experiment. The densities were determined using the final masses weighed on the ground. The results are shown in Figure 5 and summarized in Table 3 with the literature values. Moreover, detailed density values are provided as a Supplementary Material.
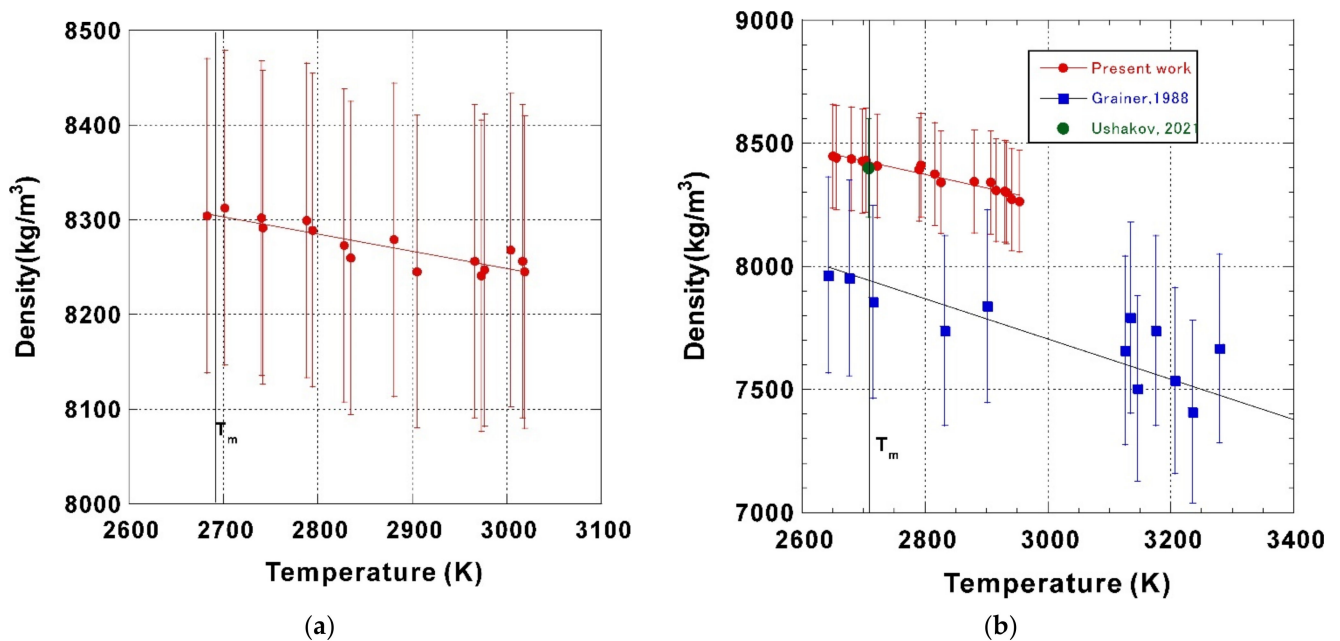

(**a**)

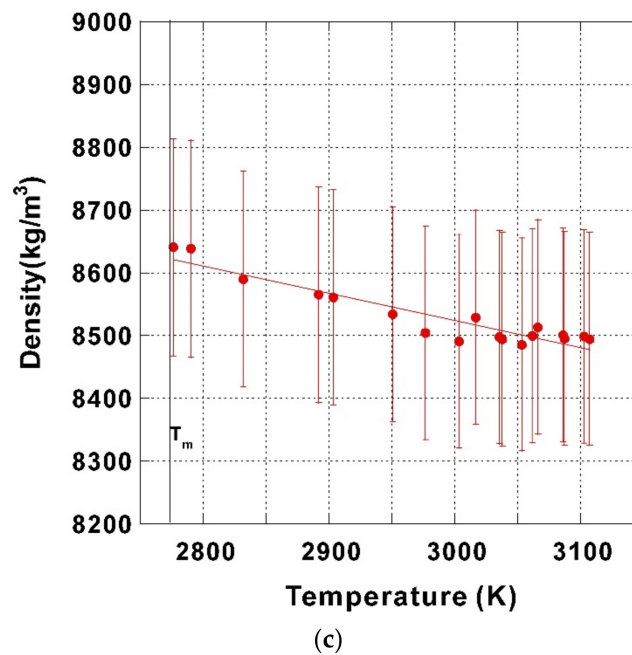(**b**)

Figure 5. *Cont.*

(**c**)

Figure 5. Measured densities of molten Ln_2O_3 vs. temperature with 2.5% error bars: (**a**) Tm_2O_3; (**b**) Yb_2O_3; (**c**) Lu_2O_3. The values by Granier and Heurtault are plotted with 5% error bars.

Table 2. Typical sample mass before and after the flight experiments.

Chemical Name	Mass before Launch (mg)	Mass after Retrieval (mg)
Tm_2O_3	17.62	17.55
Yb_2O_3	26.96	26.80
Lu_2O_3	14.62	14.62

Table 3. Measured densities at the melting temperature (ρ_m), temperature coefficients ($d\rho/dT$), and thermal expansion coefficients (β) of Tm_2O_3, Yb_2O_3, and Lu_2O_3. The literature values are also listed.

Samples	T_m (K)	r_m (kg·m^{-3})	dr/dT (kg·m^{-3}·K^{-1})	b (10^{-5}K^{-1})	Remarks
Tm_2O_3	2698 [12]	8304 ± 148	-0.18 ± 0.05	2.2 ± 0.6	Present work
Yb_2O_3	2708 [12]	8425 ± 217	-0.55 ± 0.08	6.5 ± 0.9	Present work
	2708	7940	-0.74 ± 0.13		Granier et al. [3]
	2708	8400 ± 200			Ushakov et al. [2]
Lu_2O_3	2763 [12,13]	8627 ± 240	-0.43 ± 0.08	5.0 ± 0.9	Present work

The measured densities exhibited linear behaviors as a function of temperature and could be fitted by the following equations with a confidence interval of 95%:

$$\rho_{Tm_2O_3}(T) = (8304 \pm 148) - (0.18 \pm 0.05) \times (T - T_m) \left(\text{kg·m}^{-3} \right) \tag{5}$$

$$\rho_{Yb_2O_3}(T) = (8425 \pm 217) - (0.55 \pm 0.08) \times (T - T_m) \left(\text{kg·m}^{-3} \right) \tag{6}$$

$$\rho_{Lu_2O_3}(T) = (8627 \pm 240) - (0.43 \pm 0.08) \times (T - T_m) \left(\text{kg·m}^{-3} \right) \tag{7}$$

The uncertainty of density measurements is mainly derived from the volume calculation with the image analysis. The relative uncertainty of volume ($\Delta V/V$) is [15]:

$$\frac{\Delta V}{V} = \frac{3\Delta R}{R} \tag{8}$$

A typical image of a molten Ln_2O_3 sample gives R = 120 pixels, and ΔR = 1 pixel. Therefore, the uncertainty of the density measurement is estimated to be 2.5%.

Our density value for Yb_2O_3 at its melting temperature showed a good agreement with the value reported by Ushakov et al. using an AAL [2]. The density data obtained by Granier and Heurtault with an ADL [3] were about 6% lower than our results.

These discrepancies are derived from the volume calculation from the sample image. In these three methods (AAL, ADL, and ESL), the sample volume is calculated with the assumption that the sample shape is axisymmetric. Even though it is not always true for the AAL (the sample is slightly asymmetric and experiences a slight precession [2]), good Yb_2O_3 sample images have been obtained. As for the data by Granier and Heurtault, they took the sample images from the top, from which axisymmetric sample image cannot be obtained. Therefore, the sample volumes are overestimated due to sagging. Moreover, the volumes of the sample at high temperatures would be overestimated due to their high luminosity. In our experiment, ultraviolet backlighting was employed to avoid the blurring effect of the intense infrared radiation [26]. Recently, improved ADLs with shallow nozzles have been developed so that the axisymmetrical sample image can be obtained from a horizontal view [27]. Density data measured by these improved ADLs are desired.

No reference values could be found for the densities of Tm_2O_3 and Lu_2O_3.

The thermal expansion coefficient β could be calculated by the following equation:

$$\beta = -\frac{1}{\rho(T_m)}\left(\frac{d\rho}{dT}\right) \tag{9}$$

and was listed in Table 3.

Finally, the molar volumes at the melting temperature (V_m) were calculated and compared with the values reported by Courtial and Dingwell [4] with the indirect method. The results are presented in Table 4.

Table 4. Calculated molar volumes of Tm_2O_3, Yb_2O_3, and Lu_2O_3 at the melting temperature.

Samples	Ionic Radius r (10^{-11} m)	Molar Weight m (g/mol)	Molar Volume V_m (cm³/mol)	Remarks
Tm_2O_3	8.8	385.8	46.5	Present work
			31.2	Courtial [4]
Yb_2O_3	8.68	394	46.8	Present work
			38.77	Courtial [4]
Lu_2O_3	8.61	398	46.1	Present work

Our previous work has reported that molar volumes of Ln_2O_3s (Ln = Gd, Er, Ho, and Tb) as well as those of some non-glass forming A_2O_3s (A = Al, Ga) show strong linear relations with the cube of the ionic radius (r^3) [22]. The molar volumes obtained in the present work also agree well with the relation, as shown in Figure 6.

The value for molar volume at the melting temperature of Ga_2O_3 was reported by Dingwell et al. using the double-bob method [28], whereas that of Al_2O_3 was measured by the ISS-ELF [20]. This linear relation could not be found with the scattered data (plotted in Figure 6) by the indirect method [4].

This relation suggests that their liquid atomic structures have similarities among them. The atomic structure of the Er_2O_3 melt has been measured by X-ray and neutron diffraction experiments [21]. Structural data of other Ln_2O_3 melts are currently being measured, and the similarity in their atomic structures will be evaluated.

The ISS-ELF has the capability to measure surface tension and viscosity of molten materials by the drop oscillation method [29]. Measurements of these properties on molten Ln_2O_3 are currently being conducted and will be reported later. Recently, many groups have been pursuing research with ADLs to improve density, surface tension, and viscosity

measurements of high-temperature oxide melts on the ground [27,30–34]. Our results will represent good benchmark data, helpful for furthering the development of ADLs.
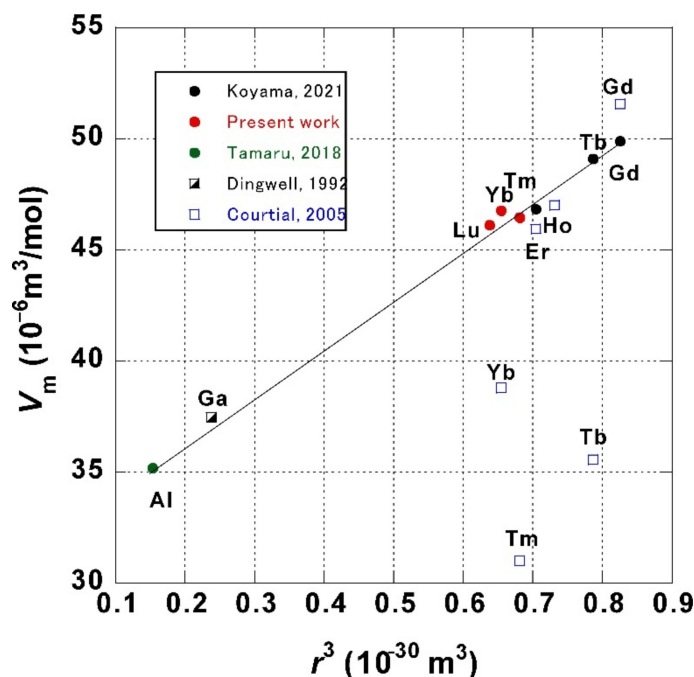

Figure 6. Molar volume of A_2O_3 at the melting temperature and relation to the cube of the ionic radius.

4. Conclusions

The densities of three molten lanthanoid sesquioxides (Tm_2O_3, Yb_2O_3, and Lu_2O_3) have been successfully measured using the ISS-ELF and exhibit a good agreement with literature values. Furthermore, their molar volumes at their melting temperatures show a clear correlation with their ionic radii, which is consistent with our previous results with Gd_2O_3, Er_2O_3, Ho_2O_3, and Tb_2O_3. Currently, JAXA's development work on the ISS-ELF focuses on the improvement in the sample position stability at elevated temperatures. This will enable the measurement of the density of ZrO_2 and HfO_2, which have melting temperatures that are higher than those of lanthanoid sesquioxides, as well as the measurement of surface tension and viscosity. These results will be reported in future publications.

References

1. Chen, Z.; Li, Z.; Li, J.; Liu, C.; Lao, C.; Fu, Y.; Liu, C.; Li, Y.; Wang, P.; He, Y. 3D printing of ceramics: A review. *J. Eur. Ceram. Soc.* **2019**, *39*, 661–687. [CrossRef]
2. Ushakov, S.V.; Niessen, J.; Quirinale, D.G.; Prieler, R.; Navrotsky, A.; Telle, R. Measurements of Density of Liquid Oxides with an Aero-Acoustic Levitator. *Materials* **2021**, *14*, 822. [CrossRef] [PubMed]
3. Granier, B.; Heurtault, S. Density of liquid rare-earth sesquioxides. *J. Am. Ceram. Soc.* **1988**, *71*, C466–C468. [CrossRef]
4. Courtial, P.; Dingwell, D.B. High-temperature density of lanthanide-bearing Na-silicate melts: Partial molar volumes for Ce_2O_3, Pr_2O_3, Nd_2O_3, Sm_2O_3, Eu_2O_3, Gd_2O_3, Tb_2O_3, Dy_2O_3, Ho_2O_3, Er_2O_3, Tm_2O_3, and Yb_2O_3. *Am. Mineral.* **2005**, *90*, 1597–1605. [CrossRef]
5. Brillo, J.; Egry, I. Density Determination of Liquid Copper, Nickel, and Their Alloys. *Int. J. Thermophys.* **2003**, *24*, 1155–1170. [CrossRef]
6. Shneider, S.; Egry, I.; Seyhan, I. Measurement of the Surface Tension of Undercooled Liquid $Ti_{90}A_{16}V_4$ by the Oscillating Drop Technique. *Int. J. Thermophys.* **2002**, *23*, 1241–1248. [CrossRef]
7. Brillo, J.; Kolland, G. Surface tension of liquid Al–Au binary alloys. *J. Mater. Sci.* **2016**, *51*, 4888–4901. [CrossRef]
8. Kobatake, H.; Fukuyama, H.; Tsukada, T.; Awaji, S. Noncontact modulated laser calorimetry in a dc magnetic field for stable and supercooled liquid silicon. *Meas. Sci. Technol.* **2010**, *21*, 025901. [CrossRef]
9. Seidel, A.; Soellner, W.; Stenzel, C. EML—An electromagnetic levitator for the International Space Station. *J. Phys. Conf. Ser.* **2011**, *327*, 012057. [CrossRef]
10. Mohr, M.; Hofmann, D.C.; Fecht, H.-J. Thermophysical Properties of an $Fe_{57.75}Ni_{19.25}Mo_{10}C_5B_8$ Glass-Forming Alloy Measured in Microgravity. *Adv. Eng. Mater.* **2021**, *23*, 2001143. [CrossRef]
11. Luo, Y.; Damaschke, B.; Schneider, S.; Lohöfer, G.; Abrosimov, N.; Czupalla, M.; Samwer, K. Contactless processing of SiGe-melts in EML under reduced gravity. *NPJ Microgravity* **2016**, *2*, 1. [CrossRef]
12. Xiao, X.; Brillo, J.; Lee, J.; Robert, W.; Hyers, R.W.; Matson, D.M. Impact of convection on the damping of an oscillating droplet during viscosity measurement using the ISS-EML facility. *NPJ Microgravity* **2021**, *7*, 36. [CrossRef]
13. Rhim, W.-K.; Collender, M.; Hyson, M.T.; Simms, W.T.; Elleman, D.D. Development of an electrostatic positioner for space material processing. *Rev. Sci. Instrum.* **1985**, *56*, 307. [CrossRef]
14. Rhim, W.-K.; Chung, S.K.; Barber, D.; Man, K.F.; Gutt, G.; Rulison, A.; Spjut, R.E. An electrostatic levitator for high-temperature containerless materials processing in 1-g. *Rev. Sci. Instrum.* **1993**, *64*, 2961. [CrossRef]
15. Chung, S.K.; Thiessen, D.B.; Rhim, W.-K. A noncontact measurement technique for the density and thermal expansion coefficient of solid and liquid materials. *Rev. Sci. Instrum.* **1996**, *67*, 3175. [CrossRef]
16. Rhim, W.-K.; Ohsaka, K.; Paradis, P.-F.; Erik Spjut, R.E. Noncontact technique for measuring surface tension and viscosity of molten materials using high temperature electrostatic levitation. *Rev. Sci. Instrum.* **1999**, *70*, 2796. [CrossRef]
17. Rulison, A.J.; Rhim, W.-K. A noncontact measurement technique for the specific heat and total hemispherical emissivity of undercooled refractory materials. *Rev. Sci. Instrum.* **1994**, *65*, 695. [CrossRef]
18. Paradis, P.-F.; Ishikawa, T.; Lee, G.-W.; Holland-Moritz, D.; Brillo, J.; Rhim, W.-K.; Okada, J.T. Materials properties measurements and particle beam interactions studies using electrostatic levitation. *Mater. Sci. Eng. R* **2014**, *76*, 1–53. [CrossRef]
19. Tamaru, H.; Koyama, C.; Saruwatari, H.; Nakamura, Y.; Ishikawa, T.; Takada, T. Status of the electrostatic levitation furnace (ELF) in the ISS-KIBO. *Microgravity Sci. Technol.* **2018**, *30*, 643–651. [CrossRef]
20. Ishikawa, T.; Koyama, C.; Saruwatari, H.; Tamaru, H.; Oda, H.; Ohshio, M.; Nakamura, Y.; Watanabe, Y.; Nakata, Y. Density of molten Gadolinium oxide measured with the electrostatic levitation furnace in the International Space Station. *High Temp. High Press.* **2020**, *49*, 5–15. [CrossRef]
21. Koyama, C.; Tahara, S.; Kohara, S.; Onodera, Y.; Småbråten, D.R.; Selbach, S.M.; Akola, J.; Ishikawa, T.; Masuno, A.; Mizuno, A.; et al. Very sharp diffraction peak in liquid Er_2O_3 with crystal-like homology. *NPG Asia Mater.* **2020**, *12*, 43. [CrossRef]
22. Koyama, C.; Ishikawa, T.; Oda, H.; Saruwatari, H.; Ueno, S.; Oshio, M.; Watanabe, Y.; Nakata, Y. Densities of liquid lanthanoid sesquioxides measured with the electrostatic levitation furnace in the ISS. *J. Am. Ceram. Soc.* **2021**, *104*, 2913–2918. [CrossRef]
23. Coutures, J.P.; Rand, M.H. Melting temperatures of refractory oxides: Part II Lanthanoid sesquioxides. *Pure Appl. Chem.* **1989**, *61*, 1461–1482. [CrossRef]
24. Sarou-Kanian, V.; Rifflet, J.-C.; Millot, F. UV-visible pyrometry of refractory oxides at high temperature. *High Temp. High Press.* **2011**, *40*, 249–261.
25. Masuno, A.; Arai, Y.; Yu, J. In situ observation of containerless solidification from undercooled Lu_2O_3 and Y_2O_3 melts. *Phase Transit.* **2008**, *81*, 553–559. [CrossRef]
26. Ishikawa, T.; Paradis, P.-F.; Yoda, S. New sample levitation initiation and imaging techniques for the processing of refractory metals with an electrostatic levitator furnace. *Rev. Sci. Instrum.* **2001**, *72*, 2490–2495. [CrossRef]
27. Langstaff, D.; Gunn, M.; Greaves, G.N.; Marsing, A.; Kargl, F. Aerodynamic levitator furnace for measuring thermophysical properties of refractory liquids. *Rev. Sci. Instrum.* **2013**, *84*, 124901. [CrossRef]
28. Dingwell, D.B. Density of Ga_2O_3 liquid. *J. Am. Ceram. Soc.* **1992**, *75*, 1656–1657. [CrossRef]
29. Ishikawa, T.; Koyama, C.; Oda, H.; Saruwatari, H.; Paradis, P.-F. Status of the Electrostatic Levitation Furnace in the ISS—Surface Tension and Viscosity measurements. *Int. J. Microgravity Sci. Appl.* **2022**, *39*, 390101. [CrossRef]

30. Hakamada, S.; Nakamura, A.; Watanabe, M.; Kargl, F. Surface Oscillation Phenomena of Aerodynamically Levitated Molten Al$_2$O$_3$. *Int. J. Microgravity Sci. Appl.* **2017**, *34*, 340403.

31. Kargl, F.; Yuan, C.; Greaves, G.N. Aerodynamic Levitation: Thermophysical Property Measurements of Liquid Oxides. *Int. J. Microgravity Sci. Appl.* **2015**, *32*, 320212. [CrossRef]

32. Kondo, T.; Muta, H.; Kurosaki, K.; Kargl, F.; Yamaji, A.; Furuya, M.; Ohishi, Y. Density and viscosity of liquid ZrO$_2$ measured by aerodynamic levitation technique. *Heliyon* **2019**, *5*, e02049. [CrossRef] [PubMed]

33. Kondo, T.; Muta, H.; Ohishi, Y. Droplet impingement method to measure the surface tension of molten zirconium oxide. *J. Nucl. Sci. Technol.* **2020**, *57*, 889–897. [CrossRef]

34. Sun, Y.; Muta, H.; Ohishi, Y. Novel method for surface tension measurement: The drop-bounce method. *Microgravity Sci. Technol.* **2021**, *33*, 32. [CrossRef]